
ICEBENCH-S2S: A BENCHMARK OF DEEP LEARNING FOR CHALLENGING SUBSEASONAL-TO-SEASONAL DAILY ARCTIC SEA ICE FORECASTING IN DEEP LATENT SPACE

A PREPRINT

Jingyi Xu^{1,*}, Shengnan Wang^{1,*}, Weidong Yang^{1,✉}, Siwei Tu¹, Lei Bai^{2,✉}, Ben Fei^{3,✉}

¹Fudan University, ²Shanghai AI Laboratory, ²Chinese University of Hong Kong

jyxu22@m.fudan.edu.cn, wdyang@fudan.edu.cn, baisanshi@gmail.com, benfei@cuhk.edu.hk

* Equal Contributions, ✉Corresponding Authors

ABSTRACT

Arctic sea ice plays a critical role in regulating Earth’s climate system, significantly influencing polar ecological stability and human activities in coastal regions. Recent advances in artificial intelligence have facilitated the development of skillful pan-Arctic sea ice forecasting systems, where data-driven approaches showcase tremendous potential to outperform conventional physics-based numerical models in terms of accuracy, computational efficiency and forecasting lead times. Despite the latest progress made by deep learning (DL) forecasting models, most of their skillful forecasting lead times are confined to daily subseasonal scale and monthly averaged values for up to six months, which drastically hinders their deployment for real-world applications, e.g., maritime routine planning for Arctic transportation and scientific investigation. Extending daily forecasts from subseasonal to seasonal (S2S) scale is scientifically crucial for operational applications. To bridge the gap between the forecasting lead time of current DL models and the significant daily S2S scale, we introduce IceBench-S2S, the first comprehensive benchmark for evaluating DL approaches in mitigating the challenge of forecasting Arctic sea ice concentration in successive 180-day periods. It proposes a generalized framework that first compresses spatial features of daily sea ice data into a deep latent space. The temporally concatenated deep features are subsequently modeled by DL-based forecasting backbones to predict the sea ice variation at S2S scale. IceBench-S2S provides a unified training and evaluation pipeline for different backbones, along with practical guidance for model selection in polar environmental monitoring tasks.

1 Introduction

Arctic sea ice, as an essential component of the Earth system, exerts profound impacts both within and beyond the pan-Arctic region Budikova [2009]. The coupled interactions between Arctic sea ice, atmosphere, and ocean influence the local weather, and the observed Arctic amplification is crucial for analyzing the global climate change Serreze and Barry [2011], Rantanen et al. [2022], Zhou et al. [2024]. Researchers have established numerical Johnson et al. [2019] and statistical models Wang et al. [2016, 2019] to simulate the dynamical properties of sea ice for short-time forecasting. However, their forecasting skills decline rapidly as forecasting leads gradually extend to the seasonal scale, primarily due to the lack of solid knowledge of physical processes Merryfield et al. [2013] and potentially inaccurate initial and boundary conditions Zhang et al. [2022]. Recent studies on adopting deep learning (DL) approaches to forecast Arctic sea ice have demonstrated promising results while circumventing the expensive computational overheads of numerical models Schneider et al. [2023]. For instance, DL-based methods have achieved skillful prediction of daily Arctic sea ice concentration (SIC) in 90 days Ren and Li [2023] and prediction of monthly sea ice extent (SIE) for the subsequent two seasons compared to dynamical and statistical methods Andersson et al. [2021]. Despite recent promising progress, the development of skillful DL models with daily forecasting lead times that transcend intra-seasonal scale is still under-explored.

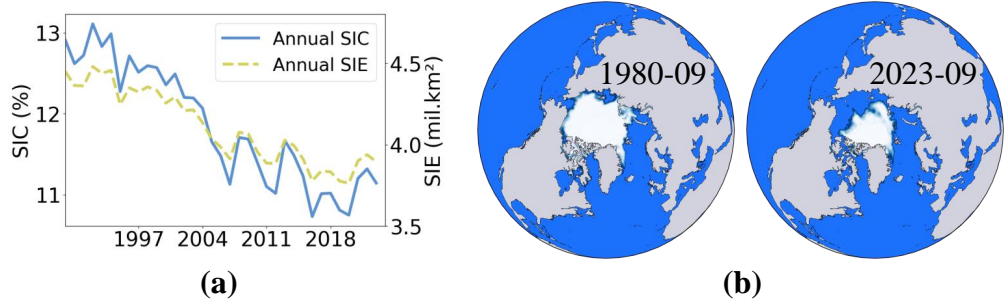


Figure 1: Variation of Arctic sea ice: (a) Annual trend of averaged Arctic sea ice concentration and sea ice extent over the last few decades. (b) Monthly average of sea ice concentration in September 1980 and 2023.

The consistent decline and negative trends of SIE during the melting season in the last few decades (as in Figure 1(a) and (b)) have opened new opportunities for Arctic maritime transportation and scientific exploration. This trend highlights the growing importance of accurate subseasonal-to-seasonal (S2S) forecasting, both for polar research Winton et al. [2022] and uncovering connections between Arctic sea ice variation and extreme weather events in middle-to-low latitudes Liu et al. [2023a]. However, significant challenges remain in extending daily forecasting lead time to inter-seasonal scale and the spring prediction barrier (SPB) of Arctic SIC before the summer season Bushuk et al. [2020]. Overcoming these limitations could further advance the development of DL-based forecasting models Ren et al. [2024]. Current DL approaches that perform at a seasonal scale mainly focus on the prediction of monthly average SIC, which inevitably fall short of forming an operational S2S Arctic sea ice forecasting system for at least two reasons: (1) The averaged monthly SIC integrates the daily variation to a coarser temporal scale and therefore neglects the nature of the temporal and spatial continuum of weather and climate Vitart and Robertson [2019]. (2) The captured monthly average pattern is useful for analyzing long-term trends, but the fine-grained information of the sea ice fluctuation is overlooked. Such absence of daily values on the inter-seasonal scale could be insufficient as a reference in real-world operations and therefore compromise the practicality of forecasting models.

To facilitate the understanding of continual long-term daily variation of Arctic sea ice, advance the operational polar research, and bridge the gap between current DL-based sea ice models and significant S2S forecasting, we introduce IceBench-S2S - the first comprehensive benchmark of a DL approach to predict daily SIC for consecutive 180 days. Inspired by previous work Zheng et al. [2024], which utilizes multivariate empirical orthogonal functions (EOFs) to compress 2D sequential daily sea ice data into time series and leverages deep neural networks for embedding and prediction, IceBench-S2S proposes a generic DL framework, namely **Sea Ice Forecasting Engine**. SIFE first compresses spatial daily sea ice data into a latent feature, then it employs DL time series models as the forecasting backbone to predict future values. By adopting this approach, IceBench-S2S could easily integrate various categories of time series DL models and comprehensively evaluate the forecasting skills of those models.

Our contributions are summarized as follows:

- We propose the first benchmark, IceBench-S2S, that focuses on the evaluation of the DL approach for daily S2S forecasting of Arctic sea ice. Thorough evaluations are conducted to investigate the potential of DL models to fulfill this challenging task.
- Motivated by prior works, we propose a generic DL framework, SIFE, that compresses daily SIC data into a deep latent space to facilitate adopting and evaluating advanced DL-based time series forecasting models.
- Our benchmark is mutually beneficial for AI and geoscience communities: the difficult S2S daily forecasting task integrated in IceBench-S2S poses significant challenges for future development of DL models; The newly constructed baselines of long-term daily SIC forecasting and our comprehensive analysis could further promote Arctic sea ice research and interdisciplinary development.

2 Related Works

Benchmarks in geoscience. Recent years have seen growing emphasis on benchmarks in geoscience, primarily addressing two key aspects Kaltenborn et al. [2023], Nguyen et al. [2023], Yu et al. [2023]. The first involves evaluating datasets (e.g., satellite products, meteorological variables) in terms of their accuracy and usability, which establishes regional validation standards Daly [2006], Loew et al. [2017]. For instance, systematic assessments of

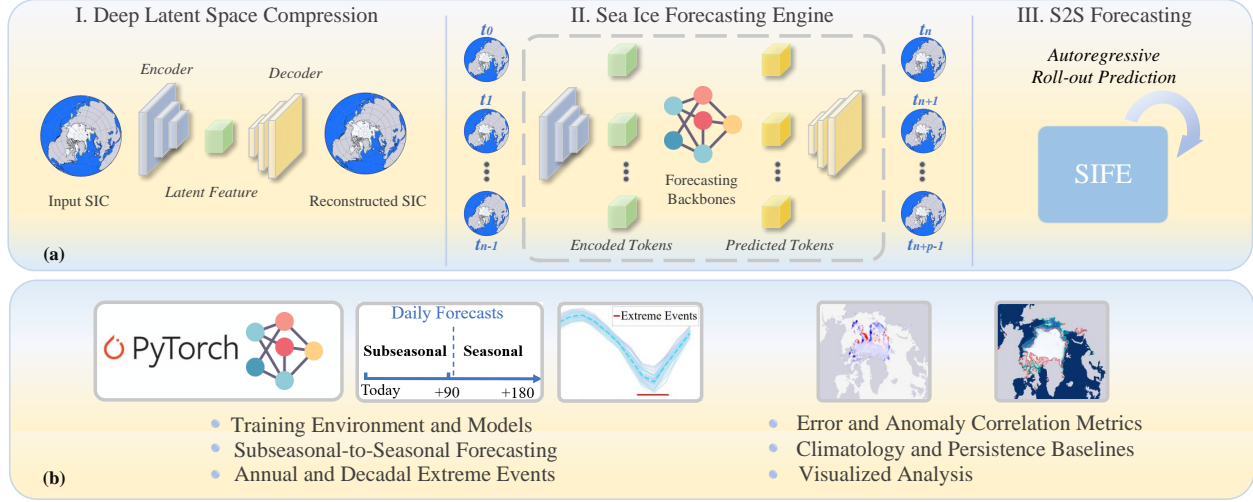


Figure 2: **IceBench-S2S.** (a) Forecasting Approach: *Deep Latent Space Compression* for spatial representation, proposed generic framework *Sea Ice Forecasting Engine* and autoregressive roll-out prediction for *S2S Arctic Sea Ice Forecasting*, n and p represent the input and predicted time steps, respectively; (b) Key components include the model *Training Environments*, challenging *Tasks*, and comprehensive *Evaluations*.

precipitation datasets like IMERG Tan et al. [2019], Huffman et al. [2015] have provided essential benchmarks for refining satellite-based hydrological models Wang et al. [2017], Pradhan et al. [2022]. The second aspect focuses on performance comparisons of forecasting models through hyperparameter optimization, such as evaluating architectures like SmaAt-Unet Trebing et al. [2021], ConvLSTM Azad et al. [2019], and DGMR Ravuri et al. [2021]. These studies aim to identify optimal configurations for specific geoscientific tasks, such as extreme rainfall prediction Suri and Azad [2024]. Regarding sea ice benchmarks, IceBench Alkaee Taleghan et al. [2025] addresses the evaluation of the sea-ice type classification problem. For the forecasting benchmark, spatially damped anomaly persistence (SDAP) Niraula and Goessling [2021], which utilizes only sea ice concentration data, was proposed to evaluate dynamical models. SDAP outperforms commonly used simple anomaly persistence and climatology baselines at subseasonal scales; its skillful seasonal forecasts compared to the best-performing dynamical forecast systems have made it a challenging benchmark method. Considering the large variability of sea ice during melting seasons, the sea ice prediction community annually hosts the Sea Ice Outlook (SIO) contribution forum to gather sea ice predictions from worldwide institutes. A comprehensive multi-model benchmark Bushuk et al. [2024] that exploits SIO prediction records was introduced to evaluate the skills of multiple dynamical and statistical models to forecast SIC and SIE in September. However, benchmark studies that specifically focus on evaluating deep learning approaches for S2S daily forecasting remain relatively scarce. In this work, we intend to bridge the gap and enrich the models in geoscience and sea ice forecasting.

Deep learning for SIC forecasting. Researchers have proposed various approaches to forecasting SIC, encompassing numerical and statistical models Wang et al. [2013], Yuan et al. [2016]. However, numerical and statistical models usually rely on high-performance computing of CPU clusters, which tends to result in complex debugging processes and uncertain parameterization. Recently, deep learning models have drawn the attention of sea ice research communities and have been widely investigated for Arctic sea ice forecasting Petrou and Tian [2019], Kim et al. [2020], Ali et al. [2021], Ali and Wang [2022]. These methods utilize U-Net-based architectures to solve daily (SICNet Ren et al. [2022]), or monthly average (IceNet Andersson et al. [2021], MT-IceNet Ali and Wang [2022]) SIC forecasting. Although these U-Net-based architectures are built on top of LSTM Liu et al. [2021], CNN Andersson et al. [2021], or vision transformer, merging channels altogether could fail to fully exploit the temporal information inherent in sea ice modeling. Moreover, these methods, including the latest Transformer-based model Zheng et al. [2024], only concentrate on single temporal granularity SIC forecasting, and their daily forecasting leads are shorter than the seasonal scale.

3 IceBench-S2S

3.1 Sea Ice Concentration Dataset

Considering the demonstrated effectiveness of leveraging SIC data to forecast future sea ice Niraula and Goessling [2021], Ren et al. [2022], we focus exclusively on SIC data for training, evaluation, and analysis in IceBench-S2S to set up S2S daily forecasting DL baselines, providing a foundation for future advancements. In IceBench-S2S, we adopt the

MSE	RMSE	MAE	NSE	ACC	R ²	PSNR	SSIM
$\frac{1}{n} \sum_{i=1}^n (y_i - \hat{y}_i)^2$	$\sqrt{\frac{1}{n} \sum_{i=1}^n (y_i - \hat{y}_i)^2}$	$\frac{1}{n} \sum_{i=1}^n y_i - \hat{y}_i $	$1 - \frac{\sum_{i=1}^n (y_i - \hat{y}_i)^2}{\sum_{i=1}^n (y_i - \bar{y})^2}$	$\frac{\frac{1}{n} \sum_{i=1}^n (\hat{y}_i - C)(y_i - C)}{\sqrt{\frac{1}{n} \sum_{i=1}^n (\hat{y}_i - C)^2} \sqrt{\frac{1}{n} \sum_{i=1}^n (y_i - C)^2}}$	$1 - \frac{\sum (y_i - \hat{y}_i)^2}{\sum (y_i - \bar{y})^2}$	$10 \log_{10} \left(\frac{\text{MAX}^2}{\text{MSE}} \right)$	$\frac{(2\mu_x\mu_y + C_1)(2\sigma_{xy} + C_2)}{(\mu_x^2 + \mu_y^2 + C_1)(\sigma_x^2 + \sigma_y^2 + C_2)}$

Table 1: Metrics utilized for IceBench evaluations.

Dataset	MSE \downarrow	MAE \downarrow	PSNR \uparrow	SSIM \uparrow	NSE \uparrow
CDR _L	0.0029	0.0123	25.35	0.9243	0.9705
CDR _S	0.0031	0.0125	25.12	0.9211	0.9689
NT _L	0.0023	0.0137	26.45	0.9048	0.9732
NT _S	0.0030	0.0163	25.31	0.8810	0.9660
BT _L	0.0026	0.0126	25.96	0.9177	0.9752
BT _S	0.0035	0.0148	24.55	0.9081	0.9650

Table 2: Compression quality of different retrieval algorithms and latent space dimensions. CDR_L, NT_L, and BT_L represent that the dimension of compressed deep latent space is 4096, while the dimension of CDR_S, NT_S, and BT_S is equal to 1024. The quality improvement of quadrupling the latent dimension is marginal.

Climate Data Record of Passive Microwave Sea Ice Concentration G02202 Version 4 dataset Meier et al. [2021] from the National Snow and Ice Data Center (NSIDC). G02202 dataset records daily SIC data starting from October 25th, 1978, and provides the coverage of the pan-Arctic region (N:89.8°, S:31.1°, E:180°, W:−180°). Each daily SIC data is formed of 448 × 304 pixels and each pixel corresponds to the area of a 25 km × 25 km grid. The SIC data has a range of 0% to 100%, and areas where the SIC value is greater than 15% indicate the SIE. G02202 contains three subsets that are generated using different retrieval algorithms: Climate Data Record (CDR) Meier et al. [2021], NASA Team (NT) Cavalieri et al. [1984], and Bootstrap (BT) Comiso [1986]. These algorithms are widely recognized in the field of sea ice concentration retrieval and are based on passive microwave remote sensing data. We utilize the CDR-retrieved SIC dataset, which is the main dataset in G02202, to train and evaluate different models. The spatial resolution of the SIC data is maintained at a size of 448 × 304. The dataset covers the period up to June 30th, 2024, spanning a total of 16,686 days. In IceBench-S2S, it is divided into three subsets as follows: training period (1979–2015), validation period (2016–2019), and testing period (2020–2024).

3.2 Task Overview

Subseasonal-to-Seasonal daily forecasting. The primary task of IceBench-S2S is to evaluate daily Arctic SIC forecasting skills on a seasonal scale, i.e., forecasting SIC for the next 180 days. Considering the dimensions of daily data and forecasting future SIC requires modeling of sequences, the S2S task poses two fundamental challenges for deep learning approaches to address: (1) *High-Dimensional Data Compression*: Effective representation of daily SIC grids that project sea ice data into deep latent space while preserving critical spatial patterns; (2) *Temporal Sequence Modeling*: Extract significant signals inherent in historical SIC data to accurately predict future daily values. We formalize the above challenges as follows:

$$\begin{aligned} \text{Compression: } & \min_{f,g} \mathbb{E}_t [\|\mathbf{X}_t - g(f(\mathbf{X}_t))\|^2], \\ \text{Forecasting: } & \hat{\mathbf{z}}_{t+\Delta} = \phi_{\text{TS}}(\mathbf{z}_{t-k:t}) \quad \Delta \in \{7, 15, 30, 180\}, \end{aligned} \quad (1)$$

where \mathbf{X}_t is daily SIC data, encoder f compress input data and decoder g restores SIC from compressed latent representation. The compression ratio $\gamma = \frac{448 \times 304}{\dim(f(\mathbf{X}_t))} \gg 1$. \mathbf{z} is the latent feature, $\mathbf{z}_{t-k:t}$ are input sequence of features and $\hat{\mathbf{z}}_{t+\Delta}$ are prediction results. ϕ_{TS} stands for the backbone of DL-based time series models. Δ is customizable for the forecasting lead time, i.e., we benchmark forecasting skills of a model in the next 7, 15, 30, and 180 days. The key requirements for DL models are as follows: (1) Maintain over 90% spatial correlation in reconstructions; (2) Ensure identical hyperparameter spaces across ϕ_{TS} implementations; (3) Evaluate temporal models through standardized protocols and commonly used metrics after spatial decoding.

Annual and decadal extreme events. The annual minimum of sea ice extent usually occurs in September, which is the end of the melting season. Accurately forecasting these annual extremes poses an additional challenge that requires models to predict both temporally and numerically align with the ground truth. Based on the analysis of trends in Figure 1(a), we pick the historical minimum SIE in September 2016 as the decadal extreme event, corresponding to the lowest annual mean of SIC since 1979. The minimum SIE in September 2022 is selected as the annual extreme event during the test set, since the annual mean SIC has drastically increased compared to previous years, indicating a potential shift in climatology.

Dataset	MSE \downarrow	MAE \downarrow	PSNR \uparrow	SSIM \uparrow	NSE \uparrow
CDR _L -NT	0.003	0.014	24.70	0.914	0.966
CDR _S -NT	0.003	0.016	24.73	0.902	0.960
CDR _L -BT	0.003	0.016	24.88	0.906	0.961
CDR _S -BT	0.004	0.014	24.25	0.909	0.962

Table 3: Robustness of learned deep latent representation. The spatial autoencoder trained on the CDR dataset performs sufficiently well on both NT and BT datasets without the need for fine-tuning.

3.3 Sea Ice Forecasting Engine

To bridge the gap between the under-explored DL-based S2S daily sea ice forecasting task, we propose the sea ice forecasting engine, **SIFE**, a generic DL framework that directly addresses the S2S daily forecasting challenges in the previous section through: (1) *Spatial Compression*: A Swin Transformer-based Liu et al. [2022a] autoencoder (Swin-AE) for spatial dimension reduction while preserving geophysical patterns; (2) *Temporal Forecasting*: Unified experimental protocols for fair comparison of various sequence forecasting backbones across different horizons, covering from subseasonal 7 days to inter-seasonal 180 days.

Deep latent space representation. The Swin-AE architecture, as in Figure 2(a).I, compresses SIC grids through hierarchical encoding and latent projection. Using Swin Transformer blocks with shifted window attention, the encoder f processes 448×304 inputs via:

$$\begin{aligned} \mathbf{X}_t^{(0)} &= \text{Conv2D}_{2 \times 2}(\mathbf{X}_t), \\ \mathbf{X}_t^{(l)} &= \text{SwinBlock}^{(l)}(\mathbf{X}_t^{(l-1)}) \quad (l = 1, \dots, 4), \end{aligned} \quad (2)$$

where $\mathbf{X}_t^{(0)} \in \mathbb{R}^{224 \times 152 \times 8}$, encoder progressively downsampling spatial dimensions by $2 \times$ per stage while doubling channels. The compressed latent code $\mathbf{z}_t \in \mathbb{R}^{1024}$ is obtained through:

$$\mathbf{z}_t = \text{MLP}(\text{Flatten}(\mathbf{X}_t^{(4)})). \quad (3)$$

The decoder g mirrors encoder operations with upsampling blocks, reconstructing $\tilde{\mathbf{X}}_t$ from \mathbf{z}_t through inverse spatial transformations. This design preserves spatial patterns with a compression ratio $\gamma = \frac{448 \times 304}{1024} = 133$.

Forecasting backbones. The compressed latent representation $\{\mathbf{z}_t\}$ are fed into temporal models to predict future variations. The collection of temporal model \mathcal{M}_{TS} in IceBench-S2S encompasses four architectural paradigms:

$$\mathcal{M}_{\text{TS}} = \begin{cases} \mathbf{a} : \text{Transformer, iTransformer, Informer, PatchTST} \\ \mathbf{b} : \text{DLinear, NLinear} \\ \mathbf{c} : \text{TimeMixer, SCInet} \\ \mathbf{d} : \text{CycleNet} \end{cases} \quad (4)$$

a. Attention-based: Transformer Vaswani [2017], iTransformer Liu et al. [2023b], Informer Zhou et al. [2021] and PatchTST Nie et al. [2023] are attention-based models. They tokenize time series data and utilize a multi-head attention mechanism for modeling sequential dependencies in the feature space. **b. Linear Baselines:** DLinear and NLinear Zeng et al. [2023] are essentially linear models. The former employs trend and seasonality decomposition and separately models those components for improved forecasting skill. The latter is more focused on adopting a normalization method to mitigate the distribution shift that is commonly observed in real-world data. **c. Multi-scale Decomposition & Hybrid:** TimeMixer Ekambaram et al. [2023] and SCInet Liu et al. [2022b] decompose time series by downscaling input data into subsequences and leveraging their interdependency to facilitate prediction. **d. Periodic Architectures:** CycleNet Lin et al. [2024] utilizes the discrete Fourier transform, a classic decomposition approach in signal processing, to explicitly identify cyclic components that could promote the performance. All models are trained under identical experimental conditions to ensure a fair comparison. They learn patterns and temporal dependencies in the compressed data to make predictions about future sea-ice states. The selection of these time series models aims to cover a wide range of approaches for predicting SIC in the compressed deep latent space and to establish a comprehensive benchmark for S2S forecasting.

Auroregressive roll-out prediction and SIFE ensembles. To achieve the consecutive 180-day forecasting lead, we adopt a rolling-based training approach that adapts time series forecasting backbones \mathcal{M}_{TS} to the S2S forecasting scenario. Considering the rolling window longer than 15 days would cause an out-of-memory issue during training of some backbones, we set the input and output length as 15 to ensure all backbones could be properly trained, i.e., SIFE autoregressively takes the 15-day prediction of its own as the input, and repeats the rolling stage 12 times to generate

Methods	7 Days						6 Months' Average						S2S (180 Days)					
	MAE ↓	R ² ↑	NSE ↑	MSE ↓	RMSE ↓	ACC ↑	MAE ↓	R ² ↑	NSE ↑	MSE ↓	RMSE ↓	ACC ↑	MAE ↓	R ² ↑	NSE ↑	MSE ↓	RMSE ↓	ACC ↑
Transformer Vaswani [2017]	0.0163	0.9215	0.9134	0.0064	0.0793	0.8165	0.0161	0.9324	0.9238	0.0064	0.0798	0.8154	0.0289	0.8298	0.8098	0.0159	0.1243	0.5405
iTransformer Liu et al. [2023b]	0.0151	0.9397	0.9332	0.0051	0.0706	0.8544	0.0169	0.9353	0.9271	0.0061	0.0778	0.8216	0.0491	0.6621	0.6239	0.0303	0.1693	0.0472
Informers Zhou et al. [2021]	0.0164	0.9253	0.9174	0.0061	0.0777	0.8202	0.0168	0.9416	0.9340	0.0060	0.0771	0.8193	0.0265	0.846	0.8283	0.0140	0.1160	0.6156
PatchTST Nie et al. [2023]	0.0128	0.9476	0.9419	0.0044	0.0661	0.8691	0.0169	0.9253	0.9157	0.0075	0.0864	0.7945	0.0224	0.8833	0.8692	0.0112	0.1051	0.6953
TimeMixer Ekambaram et al. [2023]	0.0141	0.9443	0.9382	0.0047	0.0682	0.8561	0.0196	0.9232	0.9135	0.0072	0.0846	0.7898	0.0365	0.7401	0.7108	0.0232	0.1480	0.3121
SCINet Liu et al. [2023b]	0.0161	0.9246	0.9165	0.0063	0.0787	0.8058	0.0155	0.9279	0.9188	0.0072	0.0845	0.7909	0.0170	0.9212	0.9116	0.0076	0.0867	0.8087
DLinear Lin et al. [2023]	0.0155	0.9346	0.9274	0.0055	0.0737	0.8289	0.0165	0.9317	0.9231	0.0068	0.0820	0.8194	0.0195	0.9159	0.9058	0.006	0.0886	0.7954
NLinear Zeng et al. [2023]	0.0164	0.9185	0.9108	0.0058	0.0764	0.8164	0.0178	0.9239	0.9155	0.0074	0.0859	0.8080	0.0298	0.8074	0.7838	0.0186	0.1311	0.5451
CycleNet Lin et al. [2024]	0.0143	0.9448	0.9385	0.0049	0.0691	0.8519	0.0204	0.9312	0.9224	0.0065	0.0807	0.8185	0.0511	0.6172	0.5724	0.0355	0.1842	0.3752
SIFE-Ensemble S2S Baseline	-	-	-	-	-	-	-	-	-	-	-	-	0.0175	0.9191	0.9111	0.0061	0.0776	0.8155
SDAP Niraula and Goessling [2021]	0.0071	0.9803	0.9780	0.0018	0.0424	0.9431	0.0152	0.9400	0.9331	0.0053	0.0725	0.8318	0.0230	0.8939	0.8805	0.106	0.1028	0.7320
Persistence	0.0072	0.9672	0.9672	0.0025	0.0494	0.9269	0.0536	0.5735	0.5174	0.0441	0.2049	0.0131	0.0506	0.5830	0.5307	0.0413	0.1994	0.0134
Climatology	0.0248	0.8641	0.8492	0.0117	0.1074	0.6638	0.0247	0.8643	0.8493	0.0118	0.1081	0.6733	0.0247	0.8726	0.8676	0.118	0.1085	0.6836

Table 4: Performance of SIFE with different time series forecasting backbones and the proposed baseline on the CDR dataset.

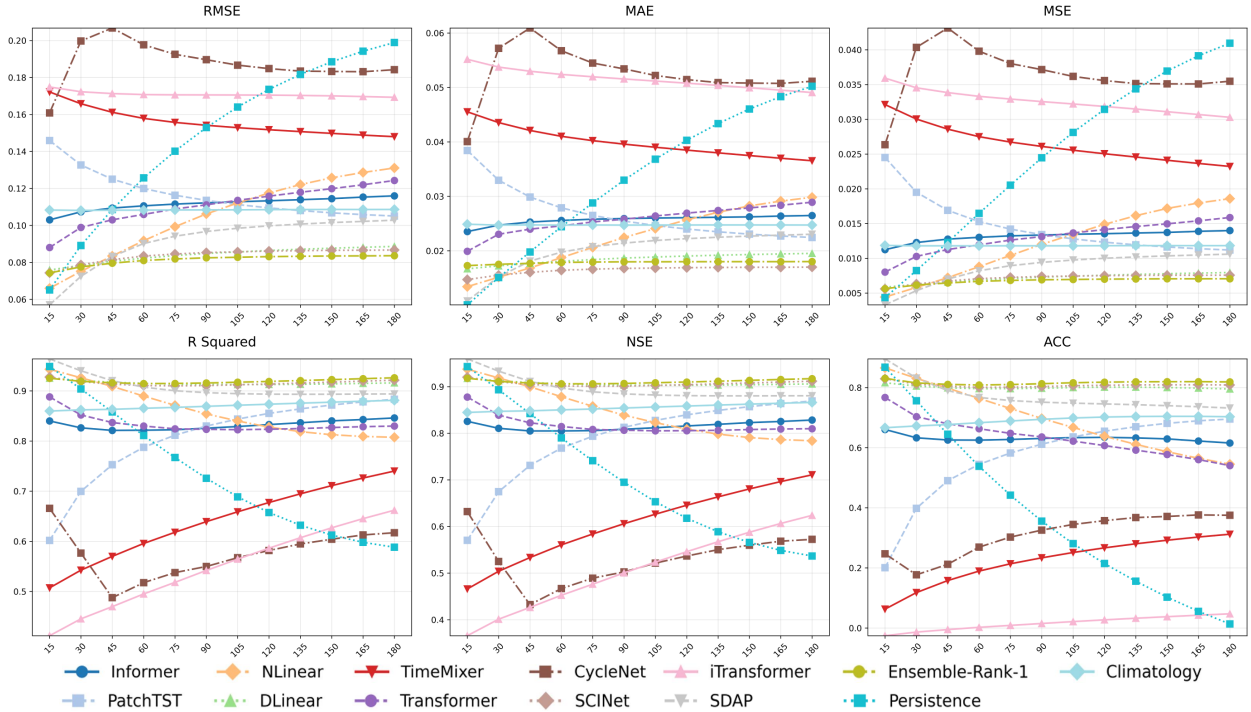


Figure 3: **Main results of S2S forecasting.** DL models along with conventional baselines, which are commonly used for validating numerical and statistical models, are evaluated under metrics outlined in Table 1 on the test dataset. Most of the DL models suffer from predictive skill loss once the forecasting lead time surpasses one month.

a total of 180 SIC forecasts. We treat the 15-day autoregressive SIFE as a recurrent neural network and leverage the teacher forcing strategy with a gradually decaying forcing ratio for a more stable training over the S2S time scale. Moreover, the model ensemble approach is exploited to form an S2S daily forecasting DL baseline.

Implementation. We implement the benchmark under a unified Python framework for impartial comparison and consistency. The PyTorch package is used for building deep neural networks with cuDNN-v9.1 and CUDA-v11.7 as the computational back-end. We are using the default setting of each forecasting backbone from the original paper. Hyperparameter settings and training details are attached to the Appendix. All experiments are performed on the same server with an NVIDIA A100 80GB GPU.

3.4 Evaluation Protocol

Research questions. We perform IceBench-S2S to explore the following: **(RQ1)** Is the proposed deep latent space representation in the SIFE framework sufficient for representing the spatial distribution of Arctic sea ice? **(RQ2)** How does the proposed SIFE compare to the previous benchmark in terms of evaluation metrics on daily, seasonal, and S2S scales? **(RQ3)** Could SIFE mitigate the Spring Prediction Barrier based solely on the SIC data and accurately forecast the September SIE?

Methods	120 Days Lead Time			90 Days Lead Time			60 Days Lead Time			30 Days Lead Time		
	RMSE (Detrend) ↓	ACC (Detrend) ↑	ACC ↑	RMSE (Detrend) ↓	ACC (Detrend) ↑	ACC ↑	RMSE (Detrend) ↓	ACC (Detrend) ↑	ACC ↑	RMSE (Detrend) ↓	ACC (Detrend) ↑	ACC ↑
Sea Ice Outlook (Sea Ice Extent)												
SIFE-S2S-Median (Fixed)	0.4425	0.5758	0.8096	0.3463	0.8061	0.8895	0.2937	0.8774	0.9207	0.1682	0.9710	0.9733
SIFE-Ensemble-Rank-1 (Fixed)	0.6030	0.5136	0.7774	0.6657	0.5173	0.7803	0.5923	0.5032	0.7695	0.6351	0.5058	0.7181
SIFE-S2S-Best (Fixed)	0.4089	0.6571	0.7960	0.3889	0.7790	0.8225	0.4050	0.7468	0.8015	0.4826	0.6119	0.8132
SIFE-S2S-Best (Finetune)	0.4036	0.6681	0.8128	0.4182	0.7662	0.8143	0.4274	0.7608	0.8187	0.4879	0.5561	0.7987
Sea Ice Outlook (Sea Ice Concentration)	0.2355	0.4310	0.4799	0.2282	0.4343	0.4971	0.2074	0.4943	0.5563	0.1518	0.6753	0.7494
SIFE-S2S-Median (Fixed)	0.3869	0.5788	0.7891	0.3646	0.6109	0.8024	0.3445	0.6483	0.8275	0.3366	0.6668	0.8270
SIFE-Ensemble-Rank-1 (Fixed)	0.3294	0.6686	0.7943	0.3148	0.6700	0.7935	0.2980	0.6762	0.7989	0.2699	0.7381	0.8398
SIFE-S2S-Best (Fixed)	0.3353	0.6644	0.7824	0.3418	0.6519	0.7720	0.3441	0.6508	0.7689	0.2879	0.7434	0.8282
SIFE-S2S-Best (Finetune)	0.2555	0.7531	0.8248	0.2540	0.7534	0.8233	0.2556	0.7571	0.8255	0.2603	0.7588	0.8250

Table 5: Performance of proposed SIFE under Sea Ice Outlook settings. Both fixed-parameter and fine-tuned SIFE demonstrate competitive forecast skill in the early spring (90 and 120 days lead time before September 1st, indicating their potential for mitigating the challenge of spring prediction barrier by only using SIC data.

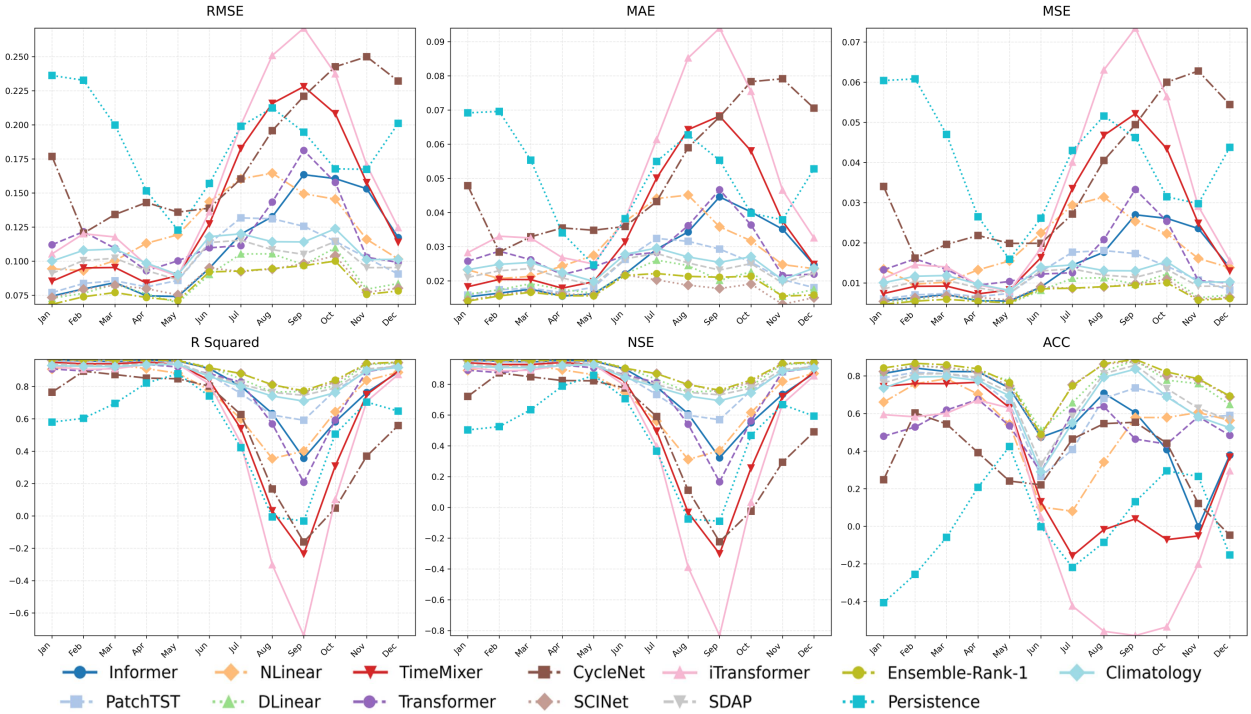


Figure 4: **S2S forecasting of calendar months over testing period.** During the melting season, when sea ice concentration fluctuates the most, the performance of all models drops abruptly, indicating the unsolved challenge of finding predictive skills throughout the summertime.

Metrics. The reconstruction quality is evaluated using five key metrics: pixel-wise accuracy, mean squared error (MSE), mean absolute error (MAE), the information-theoretic fidelity peak signal-to-noise ratio (PSNR), structural similarity (SSIM), and hydrological modeling capability Nash-Sutcliffe efficiency (NSE) Nash and Sutcliffe [1970]. These metrics collectively assess the fidelity of the reconstructed images. For the evaluation of forecasting skills, the results are assessed using MSE, MAE, the coefficient of determination (R^2), the anomaly correlation coefficient (ACC), and NSE, which provide a comprehensive overview of the models' predictive performance. All these metrics are formally defined in Table 1, where y is the ground truth SIC, \bar{y} is the spatially averaged ground truth, \hat{y} is the predicted value, and C in ACC stands for the calculated climatology.

Statistical and dynamical baselines. The commonly used persistence and climatology forecasts are calculated as simple baselines. SDAP Niraula and Goessling [2021] is implemented to represent the performance of dynamical sea ice forecasting systems. Moreover, we leverage SIO-reported predictions as a competitive baseline for evaluating the forecasting skill in the critical and challenging September.

4 Benchmark Results and Analysis

In this section, we report the primary results and analysis following the S2S forecasting task identified in the previous *Task Overview*3.2 section. Moreover, we provide extreme case studies and gain deep insight into the robustness of deep learning approaches.

4.1 Effectiveness of Latent Space Representation

To answer **RQ1**, we pre-train the encoder and decoder on the training dataset corresponding to different retrieval algorithms (CDR, NT, and BT). The test results of fidelity of reconstruction from deep latent space representation are presented in Table 2, which shows satisfactory results on test sets. The average SSIM is around 0.90, MSE is below 0.0033, and NSE is over 0.96. The result shows that the compressed representations can effectively maintain the key spatial features. On average, reducing the data dimensions from 4096 to 1024 causes a marginal 2 - 3% drop in reconstruction accuracy, which is acceptable considering the computational load it saves. Additionally, to test the robustness of the compressed latent feature, we applied the CDR-trained encoder-decoder to the NT and BT datasets. While MAE saw slight increases, the model still performed well. For example, when applying CDR_S to NT, MAE rose from 0.0125 to 0.016. Despite these minor drops, the CDR-trained encoder-decoder demonstrates good robustness by achieving relatively stable results across different datasets. The results of our robustness analysis are presented in Table 3.

4.2 S2S Forecasting Skill

Overall performance. For answering **RQ2**, we train SIFE in both a non-autoregressive and a 15-day autoregressive roll-out manner. Specifically, in the former setting, the prediction length of SIFE is set to 7 and 6, which correspond to the daily and monthly average scale. The overall performance of DL models, SDAP, persistence, and climatology baselines under the S2S forecasting scenario is given in Table 4. For a more conventional temporal scale, i.e., forecasting 7 days and 6 months' average of SIC, all DL models showcase promising results in terms of accuracy (MSE, MAE) and predictive skill (ACC, R^2). The persistence performs the best in short-term forecasting, since it assumes the state of sea ice remains in subsequent days and the variations of SIC are usually limited for a week. For the S2S forecasting scenario, it becomes more challenging for DL models. In Figure 3, we find that all DL forecasting backbones except for SCINet and DLinear suffer a severe performance drop as the forecasting lead approaches 180 days. Since DL models perform S2S forecasting in an autoregressive manner, the accumulated predictive errors inevitably compromise models' ability to capture the genuine long-term patterns. Specifically, Figure 4 showcases the primary source of error where all models perform the worst, i.e., the melting season. During the summer time, when Arctic sea ice varies the most, the loss of predictability of SIC leads to the inferior forecasting skill of DL models. However, SCINet, Informer, and DLinear models are less prone to the drop of sea ice predictability, indicating that decomposing subsequent features, modeling of long-term dependencies, and employing a combination of simple linear models could be an important factor to mitigate the challenge posed by S2S daily forecasting. To further leverage trained SIFE with different time series backbones, we explore the ensemble of different members in Table 6. After fine-tuning the ensemble weights of the top-4 performance SIFE, we find that it could further reduce the RMSE and improve the forecasting skill in terms of ACC. Hence, we propose **SIFE-Ensemble-Rank-1** as the DL baseline for S2S daily Arctic sea ice forecasting.

Sea Ice Outlook Prediction. To explore the potential of SIFE to mitigate the challenging spring barrier (**RQ3**), we introduce the SIO into our benchmark. It is a project that collects, analyzes, and synthesizes the best real-time seasonal predictions of September Arctic SIE from various institutes and agencies across the globe. It has been collecting predictions initialized on the first day of June, July, August, and added predictions initialized on September 1, providing necessary sea ice prediction information for socioeconomic activities in the Arctic region. The SIO reports forecasts from 2008 to 2021, and they can be obtained from the online repository. To evaluate the SIE and SIC forecasting skill of the SIFE, we align the forecast starting time of SIO to our test set, and compare their reported forecasts with predictions of both fixed-parameter and fine-tuned SIFE. The detailed results can be found in Table 5. The SIO clearly suffers from the SPB; their forecasting skill drops rapidly when the forecast date is earlier than May (120 days lead time), while our SIFE models are more skillful and more stable. Although the near September forecasts are less accurate than the SIO prediction, the consistent forecasting skill could indicate that our SIFE is reliable and less prone to the SPB.

15-day rolling-based strategy. To verify our strategy for a 15-day rolling window in the training stage, we compare it with a 7-day rolling window to forecast 180 days and plot the results in Figure 5. Although the backbones are identical, the average performance of 7-day forecasting models is consistently inferior to the S2S forecasting models, indicating the effectiveness of our training strategy.

SIFE-Ensembles	Members	MAE \downarrow	RMSE \downarrow	ACC \downarrow
Rank-1	Top-4	0.0175	0.0776	0.8155
Rank-2	Top-7	0.0241	0.0884	0.8100
Rank-3	All	0.0277	0.0946	0.7804

Table 6: Different backbone members in each SIFE-Ensemble rank: SCINet (R1), Informer (R1), DLinear (R1), PatchTST (R1), Transformer (R1-2), NLinear (R1-2), TimeMixer (R1-2), iTTransformer (R1-3), CycleNet (R1-3). We propose best performed model ensemble, **SIFE-Ensemble-Rank-1**, to be the DL baseline.

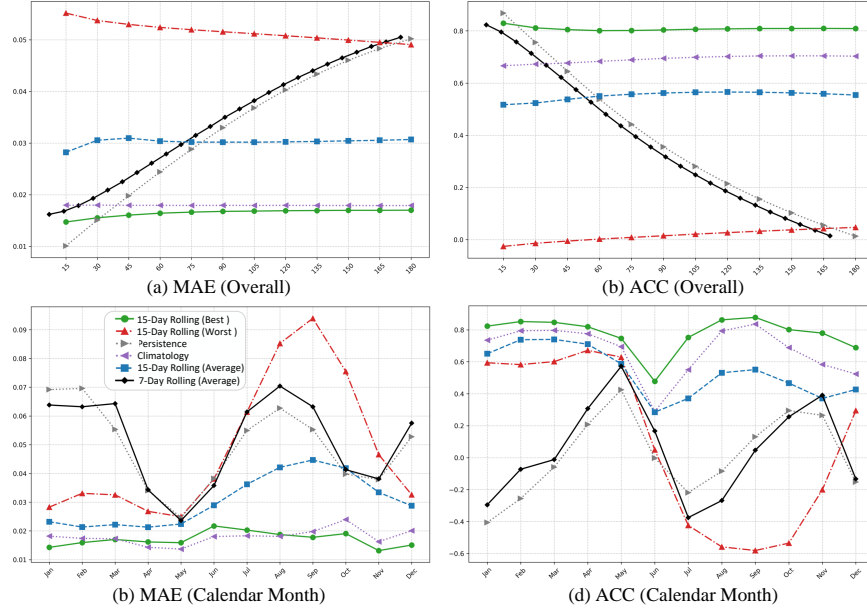


Figure 5: Comparison between S2S forecasting adopting the 7-day rolling approach and the 15-day rolling-based training strategy. The forecasting skill (ACC) of longer rolling windows is more stable than that of shorter ones.

4.3 Extreme Case Study

We present annual and decadal minimum SIE predicted by the proposed DL baseline, persistence, and climatology in Figure 6(a)-(f). Although our DL model showcases relatively superior S2S performance, predicting extreme events remains a challenging task. More visualization and residual analysis are attached to the Appendix.

5 Conclusion

We present IceBench-S2S, the first benchmark addressing the challenging and scientifically significant S2S daily sea ice forecasting. Following recent advances in climate forecasting, we perform forecasting in a deep latent space by leveraging spatial autoencoders to effectively compress daily sea ice data. Since we aim to extend daily forecasting leads from the commonly studied sub-seasonal scale to 180 days, skillful long-term time-series forecasting models are leveraged as backbones to capture sea ice variation through latent space. Our approach not only bridges the gap between sea ice forecasting and the state-of-the-art time series DL models but also forms a competitive DL baseline and poses a critical challenge for DL models to resolve. The comprehensive experiments showcase that forecasting backbones adopting subsequence decomposition and a combination of linear models could mitigate the loss of predictability during the melting seasons, indicating a potential direction for future study.

Limitation and Future Work. Considering the crucial impact posed by the Arctic sea ice, we will incorporate correlated atmospheric and oceanic variables in our future work to further investigate the potential of deep learning models for revealing fundamental atmosphere-sea-ice coupling patterns.

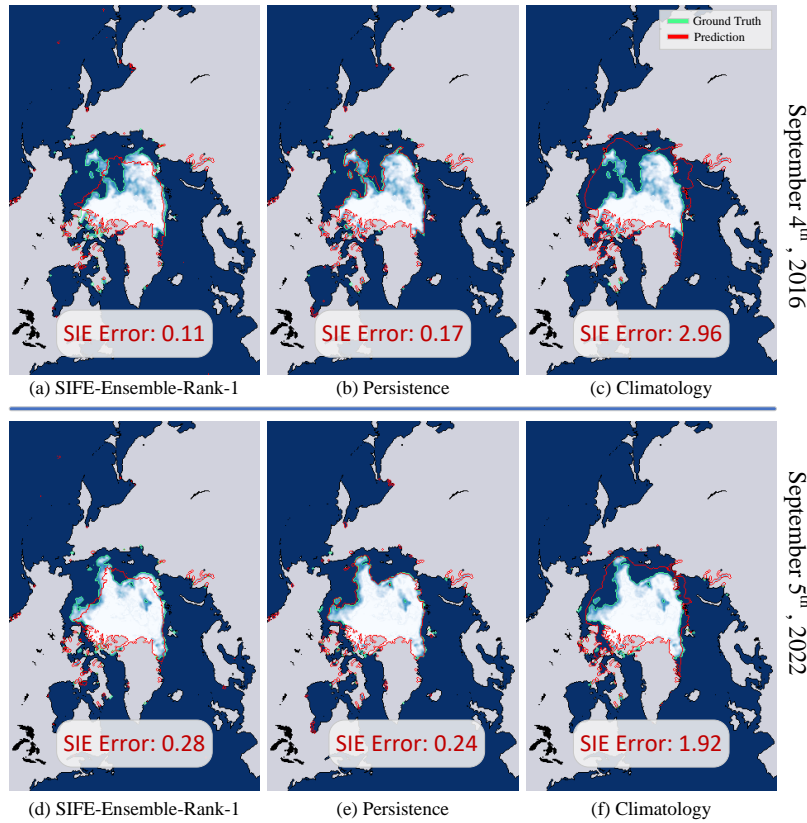


Figure 6: Observed and predicted minimum of sea ice extent in September 2016 and 2022.

References

Dagmar Budikova. Role of arctic sea ice in global atmospheric circulation: A review. *Global and Planetary Change*, 68(3):149–163, 2009. ISSN 0921-8181. doi:<https://doi.org/10.1016/j.gloplacha.2009.04.001>. URL <https://www.sciencedirect.com/science/article/pii/S0921818109000654>.

Mark C. Serreze and Roger G. Barry. Processes and impacts of arctic amplification: A research synthesis. *Global and Planetary Change*, 77(1):85–96, 2011. ISSN 0921-8181. doi:<https://doi.org/10.1016/j.gloplacha.2011.03.004>. URL <https://www.sciencedirect.com/science/article/pii/S0921818111000397>.

Mika Rantanen, Alexey Yu Karpechko, Antti Lipponen, Kalle Nordling, Otto Hyvärinen, Kimmo Ruosteenoja, Timo Vihma, and Ari Laaksonen. The arctic has warmed nearly four times faster than the globe since 1979. *Communications Earth & Environment*, 3(1):168, 2022.

W. Zhou, L.R. Leung, and J. Lu. Steady threefold arctic amplification of externally forced warming masked by natural variability. *Nat. Geosci.*, 17:508–515, 2024. doi:[10.1038/s41561-024-01441-1](https://doi.org/10.1038/s41561-024-01441-1). URL <https://doi.org/10.1038/s41561-024-01441-1>.

Stephanie J Johnson, Timothy N Stockdale, Laura Ferranti, Magdalena A Balmaseda, Franco Molteni, Linus Magnusson, Steffen Tietsche, Damien Decremer, Antje Weisheimer, Gianpaolo Balsamo, et al. Seas5: the new ecmwf seasonal forecast system. *Geoscientific Model Development*, 12(3):1087–1117, 2019.

Lei Wang, Xiaojun Yuan, Mingfang Ting, and Cuihua Li. Predicting summer arctic sea ice concentration intraseasonal variability using a vector autoregressive model. *Journal of Climate*, 29(4):1529–1543, 2016.

Lei Wang, Xiaojun Yuan, and Cuihua Li. Subseasonal forecast of arctic sea ice concentration via statistical approaches. *Climate Dynamics*, 52:4953–4971, 2019.

W. J. Merryfield, W.-S. Lee, W. Wang, M. Chen, and A. Kumar. Multi-system seasonal predictions of arctic sea ice. *Geophysical Research Letters*, 40(8):1551–1556, 2013. doi:<https://doi.org/10.1002/grl.50317>. URL <https://agupubs.onlinelibrary.wiley.com/doi/abs/10.1002/grl.50317>.

Yong-Fei Zhang, Mitchell Bushuk, Michael Winton, Bill Hurlin, Thomas Delworth, Matthew Harrison, Liwei Jia, Feiyu Lu, Anthony Rosati, and Xiaosong Yang. Subseasonal-to-seasonal arctic sea ice forecast skill improvement from sea ice concentration assimilation. *Journal of Climate*, pages 4233–4252, 2022. doi:[10.1175/JCLI-D-21-0548.1](https://doi.org/10.1175/JCLI-D-21-0548.1).

T. Schneider, S. Behera, G. Boccaletti, et al. Harnessing ai and computing to advance climate modelling and prediction. *Nat. Clim. Chang.*, 13:887–889, 2023. doi:10.1038/s41558-023-01769-3.

Yibin Ren and Xiaofeng Li. Predicting the daily sea ice concentration on a subseasonal scale of the pan-arctic during the melting season by a deep learning model. *IEEE Transactions on Geoscience and Remote Sensing*, 61:1–15, 2023.

Tom R Andersson, J Scott Hosking, María Pérez-Ortiz, Brooks Paige, Andrew Elliott, Chris Russell, Stephen Law, Daniel C Jones, Jeremy Wilkinson, Tony Phillips, et al. Seasonal arctic sea ice forecasting with probabilistic deep learning. *Nature communications*, 12(1):5124, 2021.

Michael Winton, Mitchell Bushuk, Yongfei Zhang, Bill Hurlin, Liwei Jia, Nathaniel C. Johnson, and Feiyu Lu. Prospects for seasonal prediction of summertime trans-arctic sea ice path. *Journal of Climate*, pages 4253–4263, 2022. doi:10.1175/JCLI-D-21-0634.1.

Anling Liu, Jing Yang, Qing Bao, Bian He, Xiaofei Wu, Jiping Liu, Seong-Joong Kim, and Yalan Fan. Subseasonal-to-seasonal prediction of arctic sea ice using a fully coupled dynamical ensemble forecast system. *Atmospheric Research*, 295:107014, 2023a. ISSN 0169-8095. doi:<https://doi.org/10.1016/j.atmosres.2023.107014>. URL <https://www.sciencedirect.com/science/article/pii/S0169809523004118>.

Mitchell Bushuk, Michael Winton, David B Bonan, Edward Blanchard-Wrigglesworth, and Thomas L Delworth. A mechanism for the arctic sea ice spring predictability barrier. *Geophysical Research Letters*, 47(13):e2020GL088335, 2020.

Yibin Ren, Xiaofeng Li, and Yunhe Wang. Sicnet season v1. 0: a transformer-based deep learning model for seasonal arctic sea ice prediction by integrating sea ice thickness data. *Geoscientific Model Development Discussions*, 2024: 1–20, 2024.

Frédéric Vitart and Andrew W. Robertson. Chapter 1 - introduction: Why sub-seasonal to seasonal prediction (s2s)? In Andrew W. Robertson and Frédéric Vitart, editors, *Sub-Seasonal to Seasonal Prediction*, pages 3–15. Elsevier, 2019. ISBN 978-0-12-811714-9. doi:<https://doi.org/10.1016/B978-0-12-811714-9.00001-2>. URL <https://www.sciencedirect.com/science/article/pii/B9780128117149000012>.

Qingyu Zheng, Ru Wang, Guijun Han, Wei Li, Xuan Wang, Qi Shao, Xiaobo Wu, Lige Cao, Gongfu Zhou, and Song Hu. A spatio-temporal multiscale deep learning model for subseasonal prediction of arctic sea ice. *IEEE Transactions on Geoscience and Remote Sensing*, 2024.

Julia Kaltenborn, Charlotte Lange, Venkatesh Ramesh, Philippe Brouillard, Yaniv Gurwicz, Chandni Nagda, Jakob Runge, Peer Nowack, and David Rolnick. Climateset: A large-scale climate model dataset for machine learning. *Advances in Neural Information Processing Systems*, 36:21757–21792, 2023.

Tung Nguyen, Jason Jewik, Hritik Bansal, Prakhar Sharma, and Aditya Grover. Climatelearn: Benchmarking machine learning for weather and climate modeling. *Advances in Neural Information Processing Systems*, 36:75009–75025, 2023.

Sungduk Yu, Walter Hannah, Liran Peng, Jerry Lin, Mohamed Aziz Bhouri, Ritwik Gupta, Björn Lütjens, Justus C Will, Gunnar Behrens, Julius Busecke, et al. Climsim: A large multi-scale dataset for hybrid physics-ml climate emulation. *Advances in Neural Information Processing Systems*, 36:22070–22084, 2023.

Christopher Daly. Guidelines for assessing the suitability of spatial climate data sets. *International Journal of Climatology: A Journal of the Royal Meteorological Society*, 26(6):707–721, 2006.

Alexander Loew, William Bell, Luca Brocca, Claire E Bulgin, Jörg Burdanowitz, Xavier Calbet, Reik V Donner, Darren Ghent, Alexander Gruber, Thomas Kaminski, et al. Validation practices for satellite-based earth observation data across communities. *Reviews of Geophysics*, 55(3):779–817, 2017.

Jackson Tan, George J Huffman, David T Bolvin, and Eric J Nelkin. Imerg v06: Changes to the morphing algorithm. *Journal of Atmospheric and Oceanic Technology*, 36(12):2471–2482, 2019.

George J Huffman, David T Bolvin, Dan Braithwaite, Kuolin Hsu, Robert Joyce, Pingping Xie, and Soo-Hyun Yoo. Nasa global precipitation measurement (gpm) integrated multi-satellite retrievals for gpm (imerg). *Algorithm theoretical basis document (ATBD) version*, 4(26):30, 2015.

Zhaoli Wang, Ruida Zhong, Chengguang Lai, and Jiachao Chen. Evaluation of the gpm imerg satellite-based precipitation products and the hydrological utility. *Atmospheric Research*, 196:151–163, 2017.

Rajani K Pradhan, Yannis Markonis, Mijael Rodrigo Vargas Godoy, Anahí Villalba-Pradas, Konstantinos M Andreadis, Efthymios I Nikolopoulos, Simon Michael Papalexiou, Akif Rahim, Francisco J Tapiador, and Martin Hanel. Review of gpm imerg performance: A global perspective. *Remote Sensing of Environment*, 268:112754, 2022.

Kevin Trebing, Tomasz stanczyk, and Siamak Mehrkanoon. Smaat-unet: Precipitation nowcasting using a small attention-unet architecture. *Pattern Recognition Letters*, 145:178–186, 2021.

Reza Azad, Maryam Asadi-Aghbolaghi, Mahmood Fathy, and Sergio Escalera. Bi-directional convlstm u-net with densley connected convolutions. In *Proceedings of the IEEE/CVF international conference on computer vision workshops*, pages 0–0, 2019.

Suman Ravuri, Karel Lenc, Matthew Willson, Dmitry Kangin, Remi Lam, Piotr Mirowski, Megan Fitzsimons, Maria Athanassiadou, Sheleem Kashem, Sam Madge, et al. Skilful precipitation nowcasting using deep generative models of radar. *Nature*, 597(7878):672–677, 2021.

Ankur Suri and Sarita Azad. Optimal placement of rain gauge networks in complex terrains for monitoring extreme rainfall events: a review. *Theoretical and Applied Climatology*, 155(4):2511–2521, 2024.

Samira Alkaee Taleghan, Andrew P. Barrett, Walter N. Meier, and Farnoush Banaei-Kashani. Icebench: A benchmark for deep-learning-based sea-ice type classification. *Remote Sensing*, 17(9), 2025. ISSN 2072-4292. doi:10.3390/rs17091646. URL <https://www.mdpi.com/2072-4292/17/9/1646>.

Bimochan Niraula and Helge F Goessling. Spatial damped anomaly persistence of the sea ice edge as a benchmark for dynamical forecast systems. *Journal of Geophysical Research: Oceans*, 126(12):e2021JC017784, 2021.

Mitchell Bushuk, Sahara Ali, David A Bailey, Qing Bao, Lauriane Batté, Uma S Bhatt, Edward Blanchard-Wrigglesworth, Ed Blockley, Gavin Cawley, Junhwa Chi, et al. Predicting september arctic sea ice: A multimodel seasonal skill comparison. *Bulletin of the American Meteorological Society*, 105(7):E1170–E1203, 2024.

Wanqiu Wang, Mingyue Chen, and Arun Kumar. Seasonal prediction of arctic sea ice extent from a coupled dynamical forecast system. *Monthly Weather Review*, 141(4):1375–1394, 2013.

Xiaojun Yuan, Dake Chen, Cuihua Li, Lei Wang, and Wanqiu Wang. Arctic sea ice seasonal prediction by a linear markov model. *Journal of Climate*, 29(22):8151–8173, 2016.

Zisis I Petrou and Yingli Tian. Prediction of sea ice motion with convolutional long short-term memory networks. *IEEE Transactions on Geoscience and Remote Sensing*, 57(9):6865–6876, 2019.

Young Jun Kim, Hyun-Cheol Kim, Daehyeon Han, Sanggyun Lee, and Jungho Im. Prediction of monthly arctic sea ice concentrations using satellite and reanalysis data based on convolutional neural networks. *The Cryosphere*, 14(3):1083–1104, 2020.

Sahara Ali, Yiyi Huang, Xin Huang, and Jianwu Wang. Sea ice forecasting using attention-based ensemble lstm. *arXiv preprint arXiv:2108.00853*, 2021.

Sahara Ali and Jianwu Wang. Mt-icenet-a spatial and multi-temporal deep learning model for arctic sea ice forecasting. In *2022 IEEE/ACM International Conference on Big Data Computing, Applications and Technologies (BDCAT)*, pages 1–10. IEEE, 2022.

Y Ren, X Li, and W Zhang. A data-driven deep learning model for weekly sea ice concentration prediction of the pan-arctic during the melting season. *ieee t. geosci. remote*, 60, 4304819, 2022.

Yang Liu, Laurens Bogaardt, Jisk Attema, and Wilco Hazeleger. Extended-range arctic sea ice forecast with convolutional long short-term memory networks. *Monthly Weather Review*, 149(6):1673–1693, 2021.

W.N. Meier, F. Fetterer, A.K. Windnagel, and J.S. Stewart. Noaa/nsidc climate data record of passive microwave sea ice concentration. (g02202, version 4). *National Snow and Ice Data Center*, 2021. doi:<https://doi.org/10.7265/efmz-2t65>.

D.J. Cavalieri, P. Gloersen, and W.J. Campbell. Determination of sea ice parameters with the nimbus-7 smmr. *Journal of Geophysical Research*, 89:5355–5369, 1984.

J.C. Comiso. Characteristics of arctic winter sea ice from satellite multispectral microwave observations. *Journal of Geophysical Research*, 91:975–994, 1986.

Ze Liu, Han Hu, Yutong Lin, Zhuliang Yao, Zhenda Xie, Yixuan Wei, Jia Ning, Yue Cao, Zheng Zhang, Li Dong, et al. Swin transformer v2: Scaling up capacity and resolution. In *Proceedings of the IEEE/CVF Conference on Computer Vision and Pattern Recognition*, pages 12009–12019, 2022a.

A Vaswani. Attention is all you need. *Advances in Neural Information Processing Systems*, 2017.

Yong Liu, Tengge Hu, Haoran Zhang, Haixu Wu, Shiyu Wang, Lintao Ma, and Mingsheng Long. itransformer: Inverted transformers are effective for time series forecasting. *arXiv preprint arXiv:2310.06625*, 2023b.

H. Zhou, S. Zhang, J. Peng, S. Zhang, J. Li, H. Xiong, and W. Zhang. Informer: Beyond efficient transformer for long sequence time-series forecasting. In *Proceedings of the AAAI Conference on Artificial Intelligence*, volume 35, pages 11106–11115, 2021. doi:10.1609/aaai.v35i12.17325.

Yuqi Nie, Nam H. Nguyen, Phanwadee Sinthong, and Jayant Kalagnanam. A time series is worth 64 words: Long-term forecasting with transformers. In *International Conference on Learning Representations*, 2023.

Ailing Zeng, Muxi Chen, Lei Zhang, and Qiang Xu. Are transformers effective for time series forecasting? 2023.

Vijay Ekambaram, Arindam Jati, Nam Nguyen, Phanwadee Sinthong, and Jayant Kalagnanam. Tsmixer: Lightweight mlp-mixer model for multivariate time series forecasting. In *Proceedings of the 29th ACM SIGKDD Conference on Knowledge Discovery and Data Mining*, pages 459–469, 2023.

Minhao Liu, Ailing Zeng, Muxi Chen, Zhijian Xu, Qiuxia Lai, Lingna Ma, and Qiang Xu. Scinet: time series modeling and forecasting with sample convolution and interaction. In *Proceedings of the 36th International Conference on Neural Information Processing Systems*, NIPS '22, Red Hook, NY, USA, 2022b. Curran Associates Inc. ISBN 9781713871088.

Shengsheng Lin, Weiwei Lin, Xinyi Hu, Wentai Wu, Ruichao Mo, and Haocheng Zhong. Cyclenet: Enhancing time series forecasting through modeling periodic patterns. In *Thirty-eighth Conference on Neural Information Processing Systems*, 2024.

J.E. Nash and J.V. Sutcliffe. River flow forecasting through conceptual models part i — a discussion of principles. *Journal of Hydrology*, 10(3):282–290, 1970. ISSN 0022-1694. doi:[https://doi.org/10.1016/0022-1694\(70\)90255-6](https://doi.org/10.1016/0022-1694(70)90255-6). URL <https://www.sciencedirect.com/science/article/pii/0022169470902556>.